ICAST2015 #072

Implementation of Synchronized Triple Bias-Flip Interface Circuit towards Higher Piezoelectric Energy Harvesting Capability

Yuheng Zhao, Chenbin Zhou, and Junrui Liang*

Mechatronics and Energy Transformation Laboratory (METAL)
School of Information Science and Technology
ShanghaiTech University, Shanghai, China

Abstract

It has been mathematically proved that the harvesting capability of a piezoelectric energy harvesting (PEH) system can be significantly enhanced by taking the synchronized multiple bias-flip (SMBF) strategy. Among all SMBF solutions, the parallel triple bias-flip version (P-S3BF) makes the best compromise between cost and effectiveness. This paper introduces the practical design procedures and implementation details of the P-S3BF interface circuit. The triple bias-flip operation is realized by a current-routing H-bridge, which employs six power MOSFETs for enabling the specified current flows. Experiment result shows that the P-S3BF outperforms the extensively studied synchronized switch harvesting on inductor (SSHI) and standard bridge rectifier (SEH) interface circuits under the same mechanical condition. With the piezoelectric harvester used in this experiment, P-S3BF increases the harvested power by 33%, compared to SSHI; and 300%, compared to SEH.

1. INTRODUCTION

The advancements of ultra-low-power IC technologies and energy harvesting technologies in the last decade are changing the deployment way of wireless sensor networks (WSNs). Future WSN devices can become self-powered by scavenging the energy in their ambience. The power level of existing micro-generators ranges from several microwatts to milliwatts. Three types of micro-generators have been mostly investigated for harvesting the ambient kinetic energy, i.e., electromagnetic, piezoelectric, and electrostatic generators. Among these three electromechanical transducers, the piezoelectric one can be implemented with simple configuration and provides relative high output voltage. Therefore, it is extensively studied for extracting electric power from the ambient vibration sources. There are two important emphases in the research of piezoelectric energy harvesting (PEH) systems: broadening the bandwidth and improving the energy harvesting capability. The former can be effectively achieved by mechanical methods; while the latter requires more capable designs of interface circuits.

The synchronized bias-flip (BF) interface circuits are the most extensively studied circuit solutions for enhancing the piezoelectric power conversion. They were originally designed for the vibration damping purpose [1, 2]. The first BF based energy harvesting interface circuit is called synchronized switch harvesting on inductor (SSHI). It has set a milestone for enhancing the harvesting capability by up to several folds, compared to the standard bridge rectifier (SEH), i.e., the bridge rectifier solution. The general principle of BF solutions is shown in Fig. 1(a). The voltage across the piezoelectric capacitor C_p can be rapidly changed by making use of the electrical resonance of an RLC network. By

*Corresponding author: liangjr@shanghaitech.edu.cn

synchronously flipping the piezoelectric voltage with respect to zero [1] or a dc voltage source [2] at the zero-crossing instants of the vibration velocity, the combination of C_p and the interface circuit behaves like a tunable resistance, as shown in Fig. 1(b). The power consumed by equivalent R_{conv} is regarded as the power extracted (or converted) from the piezoelectric structure. As more power is extracted from the vibrating piezoelectric structure, the electrically induced damping increases as well. The dissipated and harvested powers within the energy extraction has been further distinguished in a more detailed model, as shown in Fig. 1(c) [3]. It implies that the enhancement of energy extracting capability (corresponding to R_h+R_d) does not necessarily lead to the enhancement of energy harvesting capability (corresponding to R_h). The design principle of the PEH interface circuit should be specified as to *maximize the electrically induced damping* (increase R_h+R_d) *at low dissipative cost* (decrease R_d).

After SSHI, various BF based topologies were proposed. Ref. [4, 5] give a study on the evolution of PEH interface circuits. Some researches claimed that the harvested capability can be further enhanced by taking active intervention, i.e., pumping some amount of energy into the system in order to gain more [6, 7]. Yet, the boundary between necessary passive actions and auxiliary active actions were ambiguous until the introduction of the hybrid bias-flip solutions [8, 9, 10].

2. ACTIVE & PASSIVE BF ACTIONS

The bias-flip action can be classified into two types: active BF and passive BF, as shown in Fig. 3. The single supply pre-biasing (SSPB) [9], whose circuit and waveforms are shown in Fig.4, is taken as an example for explaining the concept of these two actions. When the equivalent current from the piezoelectric element crosses zero, two BF actions come into play. The switches S1 and S3 are turned on first. The charge stored in the capacitor C_p then flow through the storage capacitor C_r. During this action, C_r absorbs energy form the piezo-element, or more exactly from C_p. Such BF action is called *passive BF*. After the first action, the voltage across C_p becomes zero, then S1 and S3 are turned off, while S2 and S4 are turned on, which enables the storage capacitor C_r to reversely charge C_p. During this action, C_r injects energy into C_p, such that to pre-bias C_p before the start of the next half vibration cycle. Such BF action is called *active BF*.

In each BF action, the starting voltage across C_p is defined as V_b+U. By shorting C_p to an inductor L_i in series with a dc bias voltage V_b, v_p drops to V_b+γU in tens to hundreds of micro seconds due to the RLC series resonance. The flipping factor γ can be achieved within the range as follows

$$-e^{-\pi/(2Q)} \le \gamma \le 1. \tag{1}$$

Q in (1) is the quality factor of the resonant shortcut. The energy which is absorbed by V_b or injected into the piezoelectric structure from V_b is expressed as follows

$$E_{h/i,BF} = \Delta Q V_b = C_p(1-\gamma)UV_b. \tag{2}$$

ΔQ is the change of charge on C_p in each BF action. When $E_{\mathrm{h}/i,\mathrm{BF}} > 0$, the bias dc source V_b harvests energy from the piezoelectric system; when $E_{\mathrm{h}/i,\mathrm{BF}} < 0$, it injects energy into the system. The dissipated energy associated with each bias-flip action is expressed as follows

$$E_{d,BF} = \frac{1}{2}C_p(1-\gamma^2)U^2 \tag{3}$$

3. BEST BIAS-FLIP STRATEGY

Equations (2) and (3) show that, in a BF action, larger voltage change, i.e., $(1-\gamma)U$, linearly increases the extracted energy, while quadratically increases the dissipated energy. The only way to increase the extracted energy at a low dissipation cost is to *make a large voltage change by combining multiple small steps*, which leads to the proposal of SMBF interface circuits [4], as shown in Fig. 5. Mathematical analysis shows that the harvested power (normalized with respect to that in SEH) in terms of voltage variables in SMBF is

$$E_h = 2[\sum_{m=1}^{M}(1-\gamma)U_m V_{b,m} + (2-\Delta U)V_o] \tag{4}$$

Solving the zero derivative point with respect to the intermediate voltages (U_m, m=1,2,…,M) leads to the optimal bias voltages set (normalized with respect to the open-circuit voltage) as follows

$$\begin{cases} U_{m,opt} = \frac{1}{1+\gamma}, \\ \Delta U_{opt} = 1 \end{cases} \quad m = 1, 2, 3, ..., M \tag{5}$$

The normalized bias voltages in optimal P-SMBF can be derived as follows

$$V_{b,\mathrm{m}} = \frac{1-\gamma}{1+\gamma}\frac{M-2m+1}{2}, \quad \mathrm{m} = 1, 2, 3, \ldots, M \tag{6}$$

According to the derived best voltage bias-flip strategy, a new method has been discovered for the further enhancement of harvesting capability without pushing $\gamma \rightarrow -1$, that is to sophisticatedly exert more bias-flip actions, i.e., increase M, at each synchronized instant.

4. S3BF INTERFACE CIRCUIT

Fig. 6 shows the optimal voltage relays in a synchronized instant (downstairs instant) under different bias-flipping number M. Compared to the pictures of S-SMBF, the bias voltages (designated with cross marks) in the optimal P-SMBF are symmetry with respect to zero volt. In particular, in the triple bias-flips version P-S3BF, there are three bias voltages V_b, 0, and $-V_b$. Since 0 is a free voltage source, V_b and $-V_b$ can be realized with a single source and an H bridge. Therefore, the P-S3BF might be realized by using only one auxiliary voltage source V_b and some power conditioning components. Given a comprehensive consideration on the cost and effectiveness, the P-S3BF solution can make a good compromise between circuit complexity and harvesting capability enhancement. This tells the motivation of our investigation on the P-S3BF interface circuits.

The proposed P-S3BF interface circuit employs six power MOSFETs for executing the triple bias-flip actions at the zero current instants. The circuit topology is shown in Fig. 7. The circuit parameters are listed in Table I. No additional power is required for establishing the bias voltage V_b. It can be self-adaptive across the auxiliary capacitor C_b.

4.1 Operational Principle

The operational principle of P-S3BF are shown in Fig. 9. The triple bias-flip actions take place when the equivalent current i_{eq} crosses zero (or the piezoelectric cantilever is at its displacement extremes). A specific RLC resonant path is turned on at each bias-flip action, providing a shortcut for the charge

stored in C_p. Therefore, v_p can be rapidly flipped for three times with respect to the reference voltages V_b, 0, and -V_b in succession. The working phases are described as follows:

- Phase 1: $v_p>0$, *open circuit:* In this phase, the voltage across the piezo element v_p is proportional to the displacement of the piezoelectric cantilever. v_p is not high enough to get through the diode bridge ($v_p<V_o+V_F$).
- Phase 2: $v_p>0$, *constant voltage:* The diode bridge is turned on. v_p is clamped to a certain voltage, which is related to the dc load R_L. The load absorbs energy from C_p (piezoelectric structure).
- Phase 3: *downstairs,* 1^{st} *bias flip:* M_1 and M_5 are turned on. The current flow is confined in one direction by D_{L2}. The charge in C_p flows through C_b. Since V_b is positive, C_b absorbs energy in this phase. Therefore, it corresponds to a passive bias-flip action.
- Phase 4: *downstairs,* 2^{nd} *bias flip:* M_4 are turned on. The current flow is confined in one direction by D_{R1}. The charge stored in C_p flows through the resonant path with zero voltage reference. It flips v_p from positive to negative. In this phase, there is no energy change in C_b.
- Phase 5: *downstairs,* 3^{rd} *bias flip:* M_3 and M_4 are turned on. The current flow is confined in one direction by D_{R3}. In this phase, C_b reversely pumps charge to C_p. Since V_b is negative, C_b injects energy into C_p in this phase. Therefore, it corresponds to an active bias-flip action.

There are other five phases following the aforementioned five phases in the other half vibration cycle. They carry out the upstairs bias-flip actions likewise.

It is worth noting that the energy absorbed by C_b in the 1st bias flip phase and the energy injected from C_b in the 3rd bias flip phase are the same under steady state, which means that there is no energy change in C_b in one vibration cycle. The 2nd bias flip is a similar process as that in P-SSHI. The voltage across C_p changes its sign by flipping with reference to zero volt. There is also no energy change in C_b during this phase.

Enlarging the voltage amplitude across a current source yields more extracted energy; while increasing the bias-flip number and minimizing the voltage change in each step decrease the dissipated energy. These two features can be simultaneously achieved by taking the P-S3BF, therefore it can enhance the energy harvesting capability of a PEH system under the same mechanical vibration.

4.2 Current-Routing H-Bridge

There are totally six bidirectional switches for controlling the conduction or cutoff of each switching path. Each switch is realized by a diode in serial with a MOSFET (M_1 with D_{L1}, M_2 with D_{R2}, M_3 with D_{R3}, M_4 with D_{R1}, M_5 with D_{L2}, and M_6 with D_{L3}). The diode in each switching path not only helps block the voltage, but also confines the current flow in a specified direction in different bias-flip actions. The capacitor C_b in the middle of the bridge serves as the bias voltage source V_b. According to the vibration of the piezoelectric beam, V_b is able to adapt itself towards the optimal value given in (6).

4.3 Driving Circuits

The purpose of the driving circuits is to properly turn on or off the MOSFET switches with a low power consumption. Fig. 7(b) shows the driving circuit in the P-S3BF design. The switch control is delivered by a micro-controller unit (MCU). The MCU is powered by battery (the power consumption of the MCU is not considered in this study). Given the single voltage supply for powering the MCU, it can only generate positive voltage for driving the gate nodes. The low-side N-type MOSFETs (M_3 and M_6) can be directly driven by the positive voltage, yet p-type MOSFETs (M_1, M_2, M_4, and M_5) require negative gate drive voltage. An easy way to solve this problem is to design some voltage level-shifting circuits. For the high-side p-type MOSFET, taking M_1 for example, when the driving pin of the MCU,

i.e., PR1 is high, the gate and source voltages approaches V_{con} (a voltage node, rather than a source), given $R_{1b}>>R_{1a}$. When the driving pin is switched to low voltage, the gate voltage falls below V_{con}. Consequently, the negative voltage between the gate and source terminals turns M_1 on.

For the low-side p-type MOSFET, taking M_2 for example, when the driving pin of the MCU, i.e., PR2 is high, the gate and source terminals approach the ground voltage. When the driving pin is switched to low voltage, the gate voltage R2 node goes negative. A negative voltage between the gate and source terminals turns M_2 on.

With these driving circuits, all the six MOSFETs can be properly controlled by the digital I/O pins of an MCU without using the isolating gate-drive chips.

4.4 Control Timing

The control signal is provided by six I/O pins of an ultra-low-power MCU in an energy harvesting evaluation board (eZ430-RF2500, Texas Instrument, Dallas, TX). During most of the time, the MCU is in deep sleeping mode with very low maintaining current (a few μA). It only comes into operation at the bias-flip instants, such that to decrease the power consumption (this external power is not counted into the circuit dissipation in this study). The width of each gate drive pulses is half of an RLC resonance cycle

$$\Delta T = \pi\sqrt{L_i C_p}, \tag{7}$$

The switch timing control, by which the P-S3BF is activated, is shown in Fig. 8(c).

5. EXPERIMENTS

Experiments are carried out with a base excited piezoelectric energy harvester under three cases of interface circuits: SEH, P-SSHI, and P-S3BF. In each case, one of these interface circuits is connected to the piezoelectric cantilever. The actual harvested power is experimentally measured as functions of $\tilde{V}_{rect}$.

5.1 Setup

Fig. 10 shows the experimental setup. The main mechanical structure is a piezoelectric bimorph cantilever. One of its end is fixed on the shaker to form a piezoelectric cantilever. One patch of the bimorph is for energy harvesting while the other is for vibration reference. For the purpose of synchronization in both P-SSHI and P-S3BF, an electromagnetic sensor, which is composed of a coil and a pair of magnets, is installed near the free end for sensing the relative velocity of the cantilever beam. The permanent magnets also act as a proof mass at the same time. It can lower the natural frequencies and increase the displacement of the free end. The output voltage from the coil, which is proportional to the end velocity, is then input to an internal voltage comparator of the MCU. The MCU is coded to generate the switching timing accordingly for driving the six MOSFET switches, such that the synchronized bias-flip actions can be successfully carried out. The mechanical parameters are listed in Table II.

5.2 Results

Experiments are carried out for obtaining the harvested power P_h under a constant displacement magnitude harmonic excitation. Under such excitation condition, the equivalent circuit of a piezoelectric structure can be taken as a current source, thus, the mechanical effect resulting from the backward coupling can be neglected. When different dc load resistors R_L are connected one after another to stabilize the output voltage V_o at different levels, displacement magnitude is kept constant (open circuit voltage V_{oc} keeps unchanged). Once it is changed, as observed from the open-circuit voltage of the referential piezoelectric patch, the excitation amplitude is tuned for keeping the displacement magnitude to constant level.

The experimental harvested power P_h is obtained as follows

$$P_h = \frac{V_o^2}{R_L} \tag{8}$$

The non-dimensional rectified voltage $\tilde{V}_{rect}$ is defined by

$$\tilde{V}_{rect} = \frac{V_{rect}}{V_{oc}} \tag{9}$$

The rectified voltage V_{rect} is the sum of V_o and V_F, where V_F is the forward voltage drop of the bridge rectifier. It is 0.8V in the experimental circuit.

As shown in Fig. 11, the voltage profile of the P-S3BF is quite similar to P-SSHI, except those in the synchronized instants. Three stairs about the same height are observed in the triple bias-flip instants. It makes a good agreement with the theoretical prediction. As we can read from the harvested power illustrated in Fig. 12, under optimal $\tilde{V}_{rect}$, the harvested power of P-S3BF is 33% higher than P-SSHI and 300% higher than SEH in these experiments.

6. CONCLUSIONS

Given the guidance of SMBF strategy, the implementation details of P-S3BF harvesting interface circuit was introduced in this paper. The circuit operation principle were introduced in details, in order to clarify the design considerations. Some essential issues, such as the effectiveness of improvement, circuit complexity, realization of the bias voltage source, current routing, low-power control, etc. were taken into consideration towards the practical design and implementation of the P-S3BF interface circuit. Experiment results show that the harvesting capability of P-S3BF outperforms P-SSHI by 33%, which verified the capability of the SMBF strategy. Future effort should focus on the self-powered solution and the dynamic electromechanical model of the SMBF based PEH systems.

ACKNOWLEDGMENTS

The work described in this poster was supported by the grants from National Natural Science Foundation of China (Project No. 61401277) and Faculty Start-up Grant (Project No. F-0203-13-003) of ShanghaiTech University, Shanghai, China.

REFERENCES

[1] C. Richard, D. Guyomar, D. Audigier, and G. Ching, "Semi-passive damping using continuous switching of a piezoelectric device," in *Smart Structures and Materials 1999: Passive Damping and Isolation*, T. T. Hyde, Ed., vol. 3672, no. 1. SPIE, 1999, pp. 104–111.

[2] H. Ji, J. Qiu, K. Zhu, Y. Chen, and A. Badel, "Multi-modal vibration control using a synchronized switch based on a displacement switching threshold," *Smart Mater. Struct.*, vol. 18, no. 3, p. 035016, 2009.

[3] J. R. Liang and W. H. Liao, "Impedance modeling and analysis for piezoelectric energy harvesting systems," *IEEE/ASME Trans. Mechatron.*, vol. 17, no. 6, pp. 1145–1157, 2012.

[4] J. R. Liang and H. S.-H. Chung, "Best voltage bias-flipping strategy towards maximum piezoelectric power generation," *J. Phys. Conf. Ser.*, vol. 476, no. 1, p. 012025, 2013.

[5] J. Liang, "Synchronized triple bias-flips harvesting circuit: a new solution for piezoelectric energy harvesting enhancement," in *25th International Conference on Adaptive Structures and Technologies*, 2014.

[6] W. Q. Liu, Z. H. Feng, J. He, and R. B. Liu, "Maximum mechanical energy harvesting strategy for a piezoelement," *Smart Mater. Struct.*, vol. 16, no. 6, pp. 2130–2136, 2007.

[7] Y. Liu, G. Tian, Y. Wang, J. Lin, Q. Zhang, and H. F. Hofmann, "Active piezoelectric energy harvesting: general principle and experimental demonstration," *J. Intell. Mater. Syst. Struct.*, vol. 20, no. 5, pp. 575–585, 2009.

[8] M. Lallart and D. Guyomar, "Piezoelectric conversion and energy harvesting enhancement by initial energy injection," *Appl. Phys. Lett.*, vol. 97, no. 1, p. 014104, 2010.

[9] J. Dicken, P. Mitcheson, I. Stoianov, and E. Yeatman, "Power-extraction circuits for piezoelectric energy harvesters in miniature and low-power applications," *IEEE Trans. Power Electron.*, vol. 27, no. 11, pp. 4514–4529, 2012.

[10] D. Kwon and G. A. Rincon-Mora, "Energy-investment schemes for increasing output power in piezoelectric harvesters," in *IEEE 55th International Midwest Symposium on Circuits and Systems*, Aug. 2012, pp. 1084–1087.

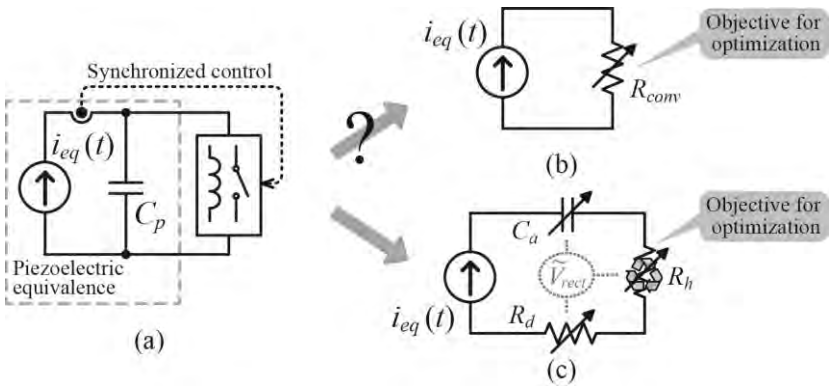

Figure 1. Bias-flip solutions for PEH. (a) Principle. (b) The equivalent targeted at power conversion (extraction). (c) The equivalent targeted at energy harvesting.

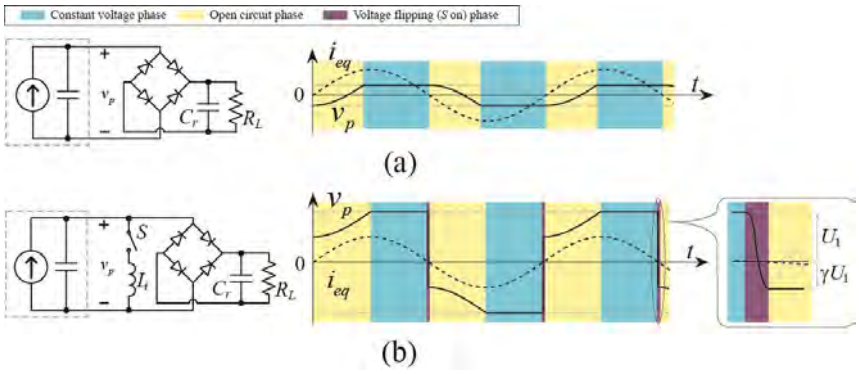

Figure 2. Circuit topologies and waveforms of two PEH interface circuits: (a) SEH. (b) P-SSHI.

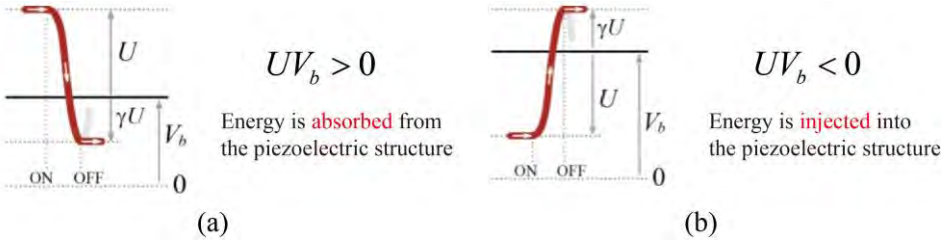

Figure 3. Bias-flip actions. (a) Passive. (b) Active.

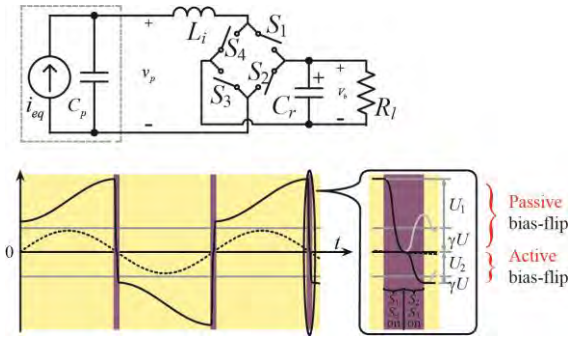

Figure 4. Circuit topology and waveform of SSPB.

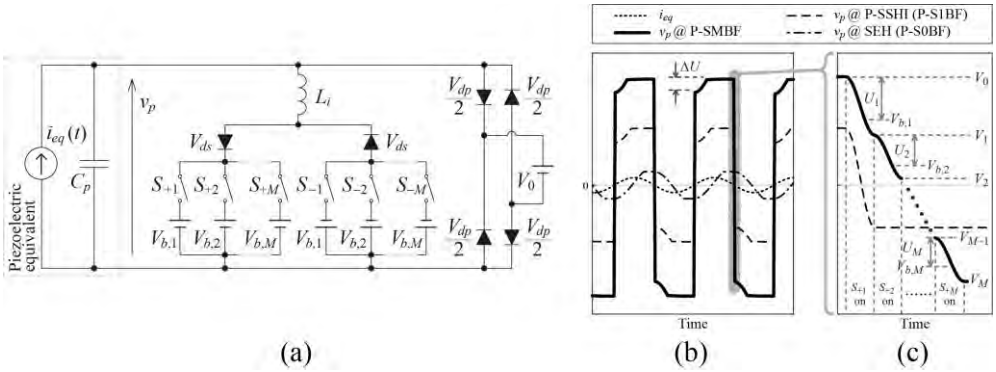

Figure 5. Generalized P-SMBF. (a) Circuit Topology. (b) Operating waveforms. (c) Zoom-in view in the synchronized instant.

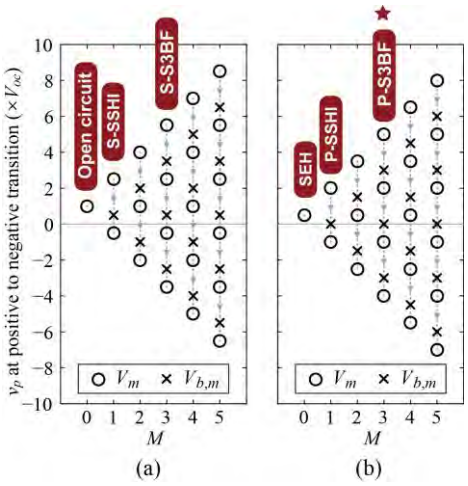

Figure 6. Optimal intermediate and bias voltages in voltage BF relay in (a) S-SMBF; and (b) P-SMBF.

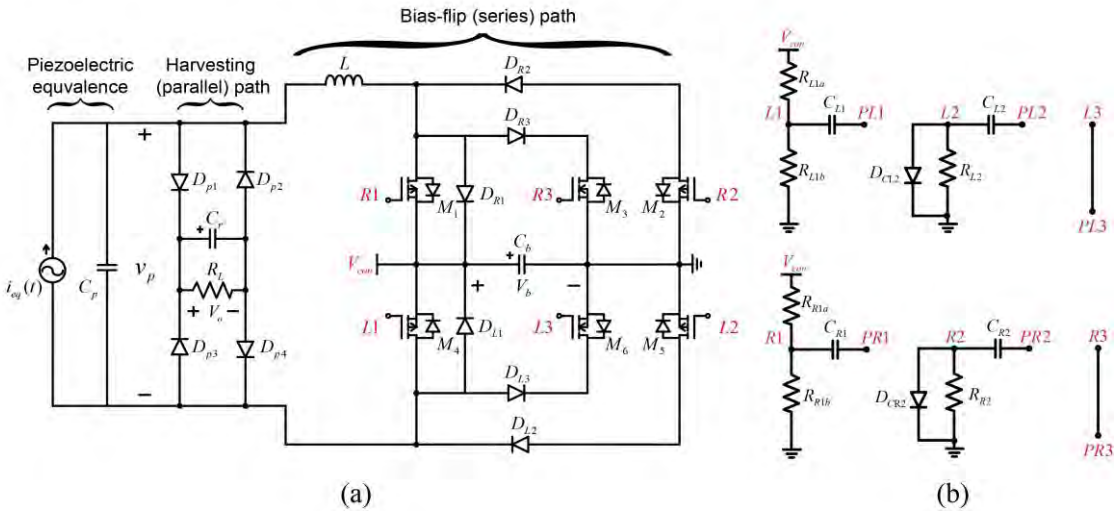

Figure 7. P-S3BF circuit. (a) Circuit topology. (b) Driving circuit.

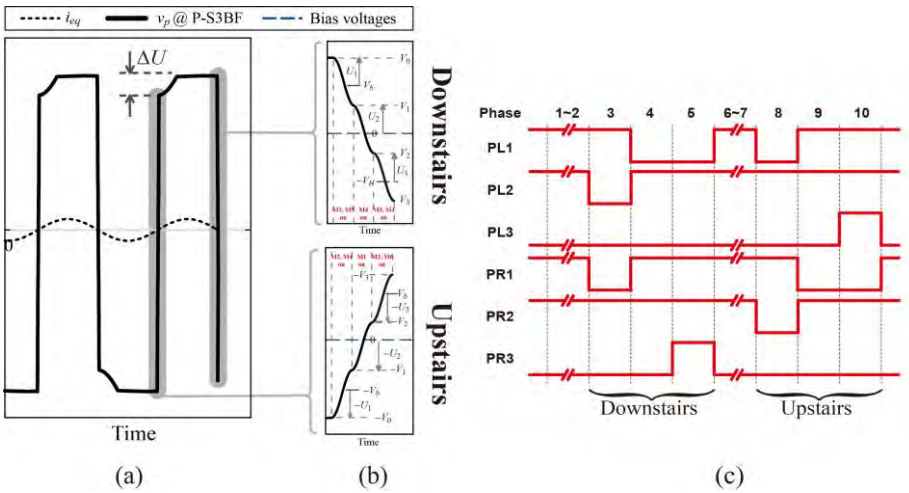

Figure 8. P-S3BF operation principle. (a) Waveforms. (b) Zoom-in view of the synchronized instant. (c) Control timing sequence.

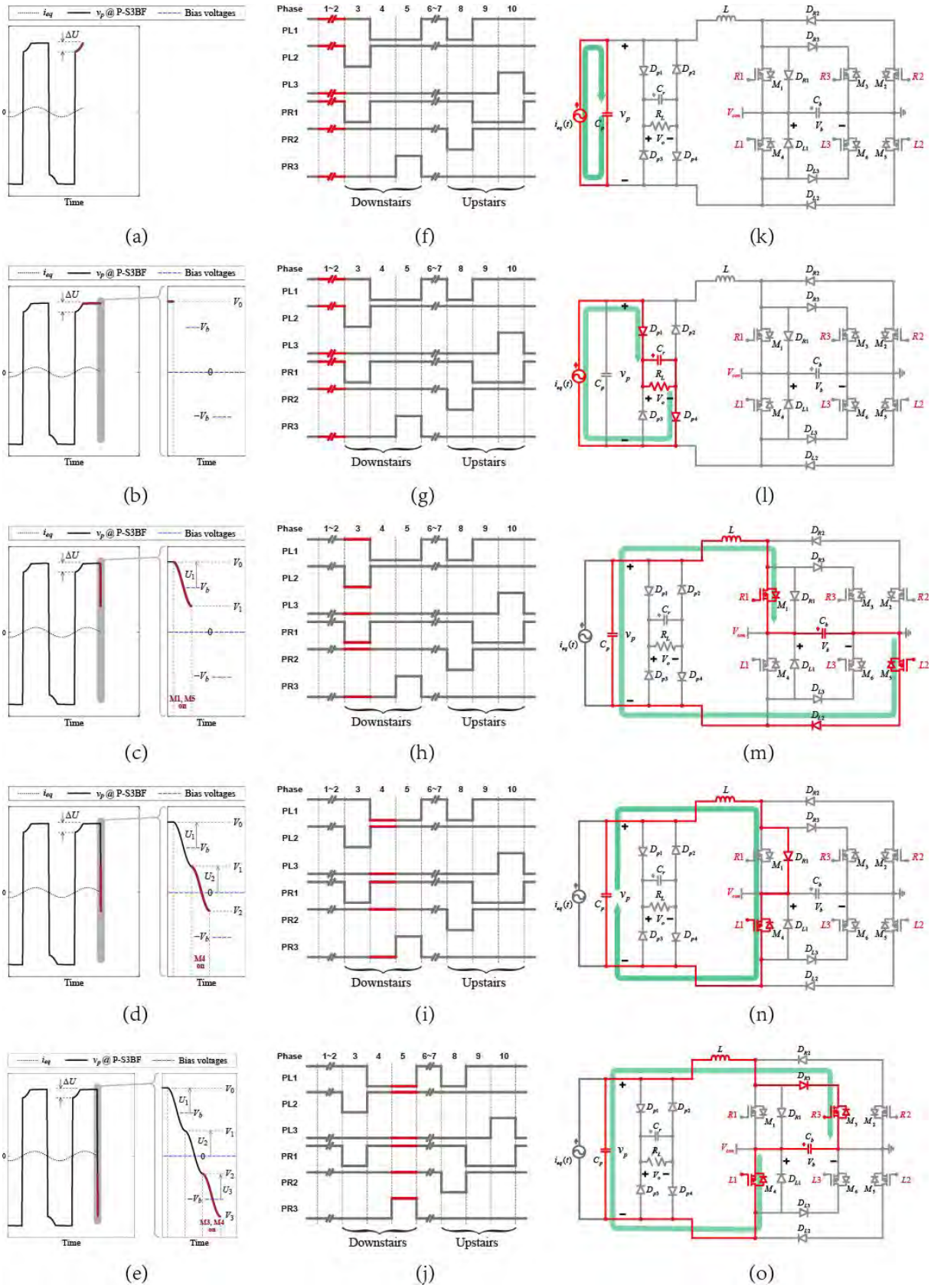

Figure 9. Working phases in half of a vibration cycle of P-S3BF. (a)-(e) Operation waveforms. (f)-(j) Control timing. (k)-(o) Current flow paths. (a) (f) (k) Open circuit. (b) (g) (l) Constant voltage. (c) (h) (m) the first bias-flip. (d) (i) (n) the second bias-flip. (e) (j) (o) the third bias-flip.

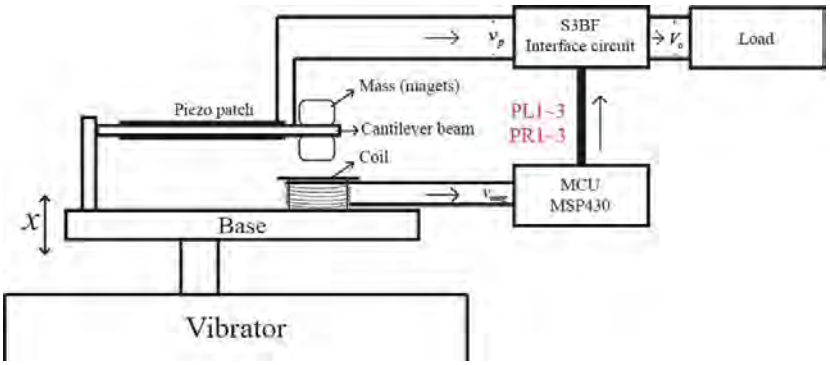

Figure 10. Experimental setup.

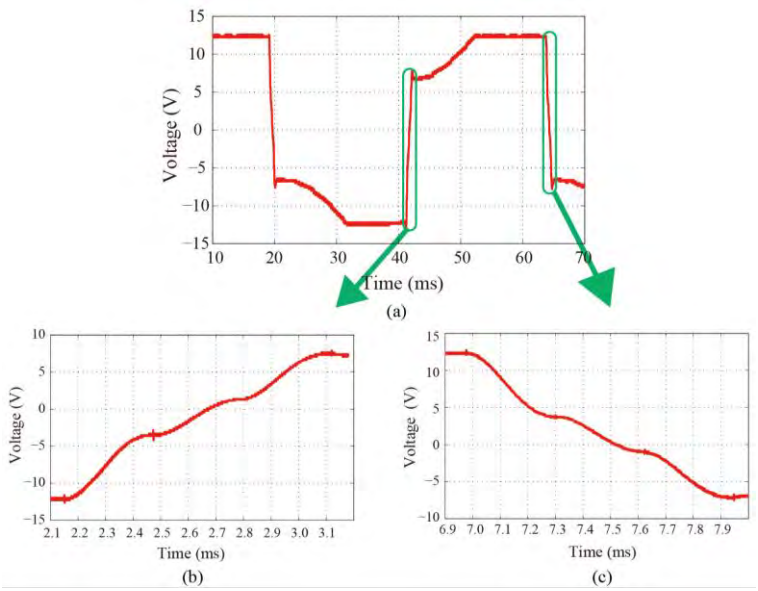

Figure 11. P-S3BF experimental result. (a) Operating waveforms. (b) Upstairs instant. (c) Downstairs instant.

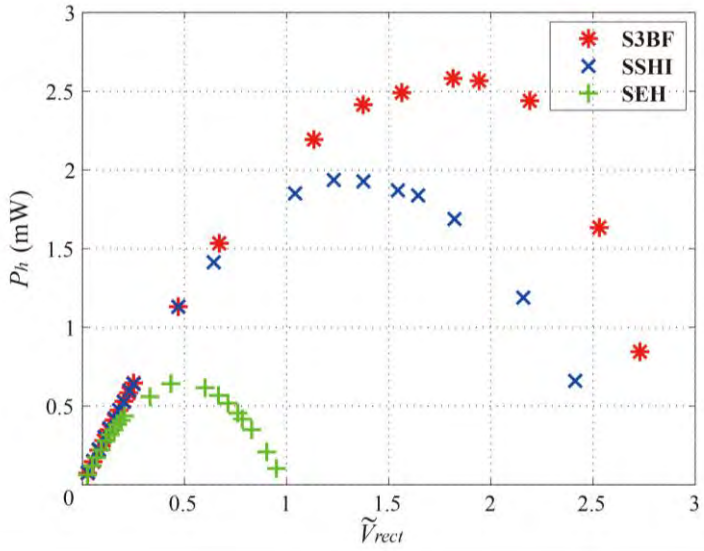

Figure 12. Harvested power by using different interface circuits.

Table 1 Electrical Specifications

Parameters	Value
Diodes	1N4004
MOSFETs	VISHAY Si4590DY
L	47 mH
Cr	33 μF
Cb	2.2 μF
R_{R1a},R_{L1a}	6.8 kΩ
R_{R1b}, R_{L1b}, R_{R2}, R_{L2}	680 kΩ
C_{L1}, C_{L2}, C_{R1}, C_{R2}	3.3 μF
γ	-0.64

Table 2 Mechanical & Piezo Specifications

Parameters	Value
Piezoelectric patch	50.0×49.7×0.2 (L×W×H) (mm)
Cantilever beam	59.5×53.1×0.2 (L×W×H) (mm)
Material	PZT-5
V_{oc}	10.75 V
C_p	220.75 nF
f_0	24.0 Hz